



This is the accepted manuscript made available via CHORUS. The article has been published as:

Superluminal math  
$$\xi(k)$$
-Gap Solitons in  
Nonlinear Photonic Time Crystals

Yiming Pan, Moshe-Ishay Cohen, and Mordechai Segev

Phys. Rev. Lett. **130**, 233801 — Published 7 June 2023

DOI: [10.1103/PhysRevLett.130.233801](https://doi.org/10.1103/PhysRevLett.130.233801)

# Superluminal k-gap solitons

## in nonlinear photonic time-crystals

Yiming Pan<sup>†1,2</sup>, Moshe-Ishay Cohen<sup>†1</sup>, Mordechai Segev<sup>1,3</sup>

1. *Physics Department and Solid State Institute, Technion, Haifa 32000, Israel*
2. *School of Physical Science and Technology and Center for Transformative Science, ShanghaiTech University, Shanghai 200031, China*
3. *Department of Electrical and Computer Engineering, Technion, Haifa 32000, Israel*

### Abstract

We propose superluminal solitons residing in the momentum gap (k-gap) of nonlinear photonic time-crystals. These gap solitons are structured as plane-waves in space while being periodically self-reconstructing wavepackets in time. The solitons emerge from modes with infinite group velocity causing superluminal evolution, which is opposite to the stationary nature of the analogous Bragg gap soliton residing at the edge of an energy gap (or a spatial gap) with zero group velocity. We explore the faster-than-light pulsed propagation of these k-gap solitons in view of Einstein's causality by introducing a truncated input seed as a precursor of signal velocity forerunner, and find that the superluminal propagation of k-gap solitons does not break causality.

Photonic time-crystals (PTCs) [1–11] are dielectric media whose permittivity ( $\epsilon$ ) is modulated periodically in time, causing time-reflected and time-refracted waves [3] to interfere, giving rise to Floquet modes associated with the momentum bands and bandgaps (also called k-gaps). PTCs seem similar to one-dimensional spatial photonic crystals (SPCs), whose dispersion is determined by periodic variation of the permittivity (Fig. 1a), with gaps where the Bloch modes have complex momentum rendering them localized in space. This analogy is misleading, as SPCs and PTCs differ in fundamental aspects. First, waves propagating in dielectric SPCs exchange momentum with the spatial lattice, conserving energy. In contrast, PTCs do not conserve energy (the modulation breaks time-translation symmetry) but conserve momentum. Second, the amplitudes of the gap modes of SPCs always decay in space, whereas the Floquet modes in the k-gap of a PTC (Fig. 1b) exhibit exponential growth (or decay) with time. The k-gap modes of PTCs exchange energy with the modulation, and their presence is related to causality (see intuitive explanation in [12]). PTCs are now drawing growing research interest [10–21], and recent experiments in epsilon-near-zero materials with very large permittivity changes within few-femtoseconds [22–29] suggests that PTCs at optical frequencies will be observed in the near future.

The momentum gap (k-gap) in PTCs suggests the existence of gap solitons, similar to those in SPCs. Gap solitons are self-trapped entities residing in the bandgap of nonlinear periodic systems such as fiber gratings [30–35] and waveguide arrays [36–42] (Fig. 1c). Gap solitons of SPCs inherit some of their features from the Bloch modes associated with the band edge in the linear system; most profoundly, they are always stationary with zero group-velocity. Is it possible to have gap solitons in the momentum gap of a nonlinear time-varying photonic media? If such k-gap solitons do exist, will they be stationary as gap solitons in SPCs, or will their group velocity be

infinite, inherited from the Floquet modes of the band edge of PTCs? Finally, if their group velocity is infinite, how can they be reconciled with causality?

Here, we find superluminal gap solitons in the momentum gap of nonlinear PTCs. These k-gap solitons are structured as finite wavepackets in time but plane waves in space. They travel faster than light, challenging special relativity, raising fundamental questions about their physical essence. We reconcile our findings with special relativity through Sommerfeld's forerunners, and suggest experiments for launching pulsed beams whose peak intensity propagates faster than light.

We begin from Maxwell's equations in nonlinear time-varying media with an instantaneous nonlinearity. For simplicity, we assume the optical Kerr effect, but the ideas are applicable to any local nonlinearity. In one-dimensional media, this yields the relation between the electric displacement  $D$  and the electric field of the light  $E$ , as  $\vec{D} = \epsilon(t, |E|^2)\vec{E} = \epsilon_0(\epsilon_1(t) + \chi^3\epsilon_0|E|^2)\vec{E}$ , with  $\chi^3$  being the Kerr coefficient. Here,  $\epsilon_1$  is the linear dielectric constant, chosen to be spatially homogeneous but periodically modulated in time  $\epsilon_1(t) = \epsilon_r(1 + \delta_1 \cos \Omega t)$ , where  $\epsilon_r$  is the mean value of the permittivity,  $\delta_1 < 1$  a small real dimensionless quantity and  $\Omega = 2\pi/T$  the modulation frequency, and  $T$  the modulation period. We assume that the medium is isotropic, drop the vector sign, and expand  $E$  in terms of  $D$  as

$$E = \frac{D}{\epsilon_0\epsilon_1} - \frac{\Gamma_3 D^3}{\epsilon_0} = \frac{D}{\epsilon_0\epsilon_1} - \frac{\chi^3 D^3}{\epsilon_0^2 \epsilon_1^4} \quad (1)$$

where we define  $\Gamma_3 = \frac{\chi^3}{\epsilon_0\epsilon_1^4}$ . From Maxwell equations, we obtain

$$\frac{\partial^2 D}{\partial t^2} = \frac{1}{\mu_0} \frac{\partial^2}{\partial x^2} \left( \frac{D}{\epsilon_0\epsilon_1} - \frac{\chi^3 D^3}{\epsilon_0^2 \epsilon_1^4} \right) \quad (2)$$

Equation (2), given in 1D, can be extended to higher dimensions, where the light is confined in all spatial dimensions but one (see Appendix). Equation (2) is different from the conventional form  $\frac{\partial^2}{\partial t^2}(\epsilon_0 \epsilon_1(t)E) = \frac{1}{\mu_0} \frac{\partial^2}{\partial x^2} E$  in terms of  $E$  [11]. We prefer  $D$  over  $E$  because, for PTC,  $D$  is continuous whereas  $E$  is not necessarily continuous. Note that  $\delta_1$  is small, so the periodic modulation has a negligible effect on the Kerr term, as long as  $\chi^3$  is small. We simplify Eq. 2 to

$$\frac{1}{c^2} \frac{\partial^2 D}{\partial t^2} = (1 - \delta_1 \cos \Omega t) \frac{\partial^2 D}{\partial x^2} - \beta |D|^2 \frac{\partial^2 D}{\partial x^2} \quad (3)$$

with the speed of light in the medium  $c = c_0/\sqrt{\epsilon_r} = c_0/n_0$ . We approximate  $\epsilon_1^{-1} = (1 - \delta_1 \cos \Omega t)/\epsilon_r$  and, in the last term only consider the contribution of the self-phase-modulation term and redefine the nonlinear coefficient  $\beta = 3\chi^3/\epsilon_0 \epsilon_r^3$ .

To obtain the k-gap soliton, we find the dispersion from (3), and derive an effective nonlinear Schrödinger-like equation (NLSE) within, or close to, the k-gap. There are several alternative treatments [32–34,43,44]; we use the nonlinear coupled-mode theory and seek solutions as the sum of suitably modulated forward and backward waves

$$D(x, t) = A_f(x, t)e^{ik_0 x - i\Omega t/2} + A_b(x, t)e^{ik_0 x + i\Omega t/2} + c. c., \quad (4)$$

with  $k_0 = \Omega/2c$ . Substituting into (3) and applying the slowly varying envelope approximation, we find that  $A_{f,b}$  obey

$$\begin{aligned} +i \left( \frac{1}{c} \frac{\partial A_f}{\partial t} + \frac{\partial A_f}{\partial x} \right) + \kappa A_b + \gamma \left( |A_f|^2 + 2|A_b|^2 \right) A_f &= 0 \\ -i \left( \frac{1}{c} \frac{\partial A_b}{\partial t} - \frac{\partial A_b}{\partial x} \right) + \kappa A_f + \gamma \left( |A_b|^2 + 2|A_f|^2 \right) A_b &= 0 \end{aligned} \quad (5)$$

With  $\kappa = \delta_1 \Omega / 8c$  being the coupling between modes and  $\gamma = \beta \Omega / 4c$  incorporating the Kerr term. If the nonlinear term has the same magnitude for the self-phase and cross-phase modulation, this equation is fully integrable and yields Manakov solitons [45–50].

**Locating the k-gap** - To find the k-gapped band, we define the two components field  $\psi$  as  $\psi = (A_f, A_b)^T$ . Seeking solutions for the linear part of (5), of the shape  $\psi = \chi e^{i(Px - Et)}$  with  $\chi$  being a spinor, we insert this ansatz into (5) for  $\gamma = 0$ , and obtain the dispersion relation

$$P(\pm) = \pm \sqrt{\left(\frac{E}{c}\right)^2 + \kappa^2} \quad (6)$$

As expected from [11], there is a momentum gap (“k-gap”) for  $|P| < \kappa$ . The k-gapped band is plotted in Fig. 1c, where the sign  $\pm$  denotes upper and lower branches. To investigate the group velocity and the group velocity dispersion (GVD) around the band edge of the k-gap, we choose a point  $(E_0 + \frac{\Omega}{2}, P_0 + k_0)$  on the band, and expand the dispersion (6) around it to the second-order

$$v_g^{(\pm)} = \left(\frac{\partial P^{(\pm)}}{\partial E}\right)^{-1} = \pm \left(\frac{\sqrt{\left(\frac{E_0}{c}\right)^2 + \kappa^2}}{\frac{E_0}{c}}\right) c \quad , \quad \text{GVD}^{(\pm)} = \left(\frac{\partial^2 P^{(\pm)}}{\partial E^2}\right) = \pm \frac{1}{c^2 \sqrt{\left(\frac{E_0}{c}\right)^2 + \kappa^2}} \quad (7)$$

Note that the group velocity  $v_g^{(\pm)}$  becomes infinite as  $E_0$  goes to 0 (when the frequency goes to half the modulation frequency  $\omega \rightarrow \Omega/2$ ) indicating that any physical solution around the bandgap must be a moving solution. Thus, the energy carried by the soliton should (seemingly) travel faster than light (Fig. 1d). This raises the question of whether the k-gap solitons are superluminal and how can this be reconciled with special relativity. As we show later, k-gap solitons are indeed superluminal (Fig. 1b). Second, the group velocity dispersion (GVD) is nonzero at the band edges:  $\text{GVD}^{(\pm)} = \pm 1/\kappa c^2 = \pm 8/\delta_1 \Omega c$ . Thus, even though the modes around the band edge are

superluminal, they still experience dispersive effects. Namely, even though the first derivative of the dispersion relation is infinite, the second derivative plays an important role, and as shown below its presence is crucial to the formation of k-gap solitons. The sign of the GVD denotes normal / anomalous dispersion. Accordingly, the spinor eigenvectors  $\chi^{(\pm)}$  associated with  $P_{\pm}$  are,

$$\chi^{(+)} = \left( \frac{\sqrt{\frac{E^2}{c^2} + \kappa^2} - \frac{E}{c}}{2(\frac{E^2}{c^2} + \kappa^2)} \right)^{1/2} \begin{pmatrix} \frac{\kappa}{\sqrt{\frac{E^2}{c^2} + \kappa^2} - \frac{E}{c}} \\ -1 \end{pmatrix} \equiv \begin{pmatrix} \chi_1^{(+)} \\ \chi_2^{(+)} \end{pmatrix}; \quad \chi^{(-)} = \left( \frac{\sqrt{\frac{E^2}{c^2} + \kappa^2} - \frac{E}{c}}{2(\frac{E^2}{c^2} + \kappa^2)} \right)^{1/2} \begin{pmatrix} 1 \\ \frac{\kappa}{\sqrt{\frac{E^2}{c^2} + \kappa^2} - \frac{E}{c}} \end{pmatrix} \equiv \begin{pmatrix} \chi_1^{(-)} \\ \chi_2^{(-)} \end{pmatrix} \quad (8)$$

Note the normalization  $\chi^{(+)}\chi^{(+)} = \chi^{(-)}\chi^{(-)} = 1$  and the orthogonality  $\chi^{(+)}\chi^{(-)} = 0$ . The solutions at the band edges are of the form  $\chi^{(+)} = (1, -1)^T / \sqrt{2}$  for the upper branch, and  $\chi^{(-)} = (1, 1)^T / \sqrt{2}$  for the lower branch. These solutions can be described as a wave that does not move at all, and all points in space have the same amplitude at any given time, but the amplitude oscillates in time at half the modulation frequency with  $D^{(-)} = e^{iP^{(-)}x} \cos\left(\frac{\Omega t}{2}\right)$ , and  $D^{(+)} = e^{iP^{(+)}x} \sin\left(\frac{\Omega t}{2}\right)$ . Henceforth we present the lower-branch k-gap solitons, while the upper branch solitons are discussed in the Supplementary Material.

**Solitons in the k-gap.** Next, we derive the NLSE from the equations (5). For the lower band branch (-), we seek solutions of the form  $\psi = a(x, t)\chi^{(-)}e^{e^{i(-P_0x - E_0t)}}$  with  $P_0 = \left(\left(\frac{E_0}{c}\right)^2 + \kappa^2\right)^{1/2}$ .

Substituting (8) into (5), we obtain the NLSE for the slowly varying amplitude  $a(x, t)$ ,

$$\left(-i \frac{\partial}{\partial x} - \frac{i}{v_g} \frac{\partial}{\partial t} - \frac{\text{GVD}}{2} \frac{\partial^2}{\partial t^2}\right) a + \alpha |a|^2 a = 0 \quad (9)$$

where  $\alpha = \gamma \left(3 - \frac{E_0/c}{E_0^2/c^2 + \kappa^2}\right) / 2$ . To solve (9), we substitute  $T = t - \frac{x}{v_g}$ ,  $X = x$ , and obtain the

standard form  $\left(-i \frac{\partial}{\partial X} - \frac{\text{GVD}}{2} \frac{\partial^2}{\partial T^2}\right) a + \alpha |a|^2 a = 0$ . Notice that in (7),  $\text{GVD} < 0$  for the lower

branch (-), hence to construct a bright soliton we need a focusing Kerr nonlinearity  $\alpha > 0$  [37,39,41]. Otherwise, we would obtain dark k-gap solitons. The bright soliton solution for (9) is  $a = u_0 \operatorname{sech}\left(\frac{t}{\tau_0}\right) e^{iqx} = u_0 \operatorname{sech}\left(\frac{t-x/v_g}{\tau_0}\right) e^{iqx}$ , with  $\tau_0 = \tau_0(u_0) = \frac{1}{u_0} \left(\frac{|GVD|}{\alpha}\right)^{1/2}$ ,  $q = q(u_0) = \frac{\alpha u_0^2}{2}$ . Thus, we obtain the soliton spinor wavefunction  $\psi = u_0 \operatorname{sech}\left(\frac{t-x/v_g}{\tau_0}\right) \chi^{(-)} e^{i(-P_0+q)x} e^{-iE_0 t}$ , and the corresponding electric displacement vector (4), at the band edge ( $E_0 \rightarrow 0$ ), with parameters  $1/v_g = 0$ ,  $|GVD| = \frac{1}{\kappa c^2}$ ,  $\alpha = \frac{3\gamma}{2}$ ,  $\tau_0 = \frac{1}{cu_0} \sqrt{\frac{2}{3\gamma\kappa}}$ ,  $q = \frac{3\gamma u_0^2}{4}$  and  $\chi_1^{(-)} = \frac{1}{\sqrt{2}}$ ,  $\chi_2^{(-)} = \frac{1}{\sqrt{2}}$ . The bright k-gap soliton of the lower branch is

$$D(x, t) = \frac{2u_0}{\sqrt{2}} \operatorname{sech}\left(\frac{t}{\tau_0}\right) \left( \cos\left(kx - \frac{\Omega t}{2}\right) + \cos\left(kx + \frac{\Omega t}{2}\right) \right) \quad (10)$$

where  $u_0$  is the peak amplitude,  $k = k_0 - \kappa + q = k_0 - \kappa + \frac{3|\gamma|u_0^2}{4}$  is the effective intensity-induced wavevector,  $\kappa$  is the strength of the coupling determining the width of the momentum gap, and  $\gamma$  incorporates the Kerr term.

To observe k-gap solitons in experiments, it is useful to confine the medium in a waveguide. Thus, we extend the analysis to higher dimensions (see Appendix). The soliton (10) offers many interesting effects. First, the k-gap soliton has the temporal form  $\operatorname{sech}(t/\tau_0)$ , as shown in Fig. 1d, but no spatial dependence. Second, the k-gap soliton differs from the stationary Bragg solitons in the  $\omega$ -gap [30–35] (Fig. 1b), due to the infinite group velocity they inherit from the Floquet modes at the band edge of the k-gap. Let us elaborate. Stationary Bragg solitons occur in nonlinear periodic systems, such as optical fibers with grating imprinted in them or in photonic lattices. These Bragg systems conserve energy. The solitons arise from the modes residing in the gap (of the linear system) which are exponentially-decaying with complex wavenumbers, as the

exponentially-diverging solution is nonphysical. The group velocity of the Bloch waves in the gap is zero. Hence, the Bragg solitons, which arise from the gap modes, inherit the zero group-velocity, and maintain the position of their peak amplitudes as they evolve. In contradistinction, our k-gap solitons conserve momentum instead of energy, and the gap modes of PTCs (of complex energies) support exponentially-growing modes, unlike the energy-conserving Bragg solitons. Fourth, the k-gap soliton comprises of two counterpropagating pulses generated simultaneously due to the momentum conservation in PTCs [12,15]. The electromagnetic field of the soliton is oscillating at frequency and wavevector:  $\omega = \frac{\Omega}{2}$ ,  $k = k_0 - \kappa + \frac{3|\gamma|u_0^2}{4} \in k\text{-gap}$ . Thus, the soliton oscillates at a frequency locked at  $\Omega/2$ , but its wavenumber can be anywhere in the gap.

Finally, the intensity of the soliton decreases monotonically in time after it reaches its peak. This is surprising, as in a linear PTC the growing mode usually dominates the dynamics. The nonlinearity leads to transfer of power from the growing modes to the decaying modes. As the intensity goes down, any slight variation in the state injects energy back to the growing mode, resulting in an infinite train of solitons that are equally spaced in time and do not interact. This train of k-gap solitons emerges naturally under almost any initial conditions, extracting energy from the modulation. The periodically emerging solitons do not interact with one another because their creation does not arise from nonlinear instability (as it does for bright Kerr solitons, where the nonlinearity drives the instability). Rather, in PTCs, the instability comes from the linear part of the system, and the nonlinearity acts as a restraining mechanism instead of a source of instability. The emergence of such a train of k-gap solitons is further discussed in the Supplementary Material.

Proceeding to the upper branch (+), we obtain k-gap solitons for defocusing nonlinearity ( $\gamma < 0$ )

$$D(x, t) = \sqrt{2}u_0 \operatorname{sech}\left(\frac{t}{\tau_0}\right) \left( \cos\left((k_0 + \kappa - q)x - \frac{\Omega t}{2}\right) - \cos\left((k_0 + \kappa - q)x + \frac{\Omega t}{2}\right) \right) \quad (11)$$

where the frequency and wavevector conform with the ‘linear’ k-gap,  $\omega = \frac{\Omega}{2}$ ,  $k = k_0 - \kappa + q = k_0 - \kappa + \frac{3|\gamma|u_0^2}{4} \in k\text{-gap}$ . The detailed derivations are given in the Supplementary Material.

**Generating k-gap solitons from a localized input.** The k-gap soliton is self-trapped in time but uniform and infinite in space. This raises a natural question on how to generate a k-gap soliton from a finite input beam. This issue is highlighted by the superluminality of the k-gap soliton. Thus, we simulate the evolution of the k-gap soliton from a finite input "seed" beam with a limited bandwidth. We launch a weak Gaussian beam into the nonlinear PTC, with all its k-components in the k-gap, and solve the Eq. (3) numerically. Figure 2(a-c) presents the evolution of three input beams with spatial width ranging from narrow to wide.

Initially, the weak input beam associated with the k-gap exhibits exponential growth in time but no propagation dynamics. The growing field is dominated by the k-gap-induced amplification with a fixed subharmonic frequency ( $\Omega/2$ ). As time progresses, the growing field becomes strong, and the nonlinearity comes into play. The intensity growth is arrested because the band structure changes (through the nonlinear interaction) such that the wavepacket resides in the band rather than in the gap (See SM). Once reaching maximal intensity, the peak splits into two counterpropagating wavepackets [3], and travels at superluminal velocity (Fig. 2). The field at different positions reaches the intensity apex at different times, and we can track the envelope trajectory and define an effective group velocity. This field envelope preserves its temporal soliton-like shape with group velocity exceeding the speed of light in the medium (Fig. 2d and videos in SM), making it superluminal in the sense that "its center of mass" (i.e. the intensity-

weighted average position of the soliton, quantity well correlated with the peak of the beam) propagates faster than light, that is, faster than the effective speed of light in the PTC ( $c/n_{eff}$ ).

Figure 2d presents the temporal profiles at different positions for the simulation presented in Fig. 2b. We estimate that the superluminal apex propagation from  $x = 0$  to  $x = 200cT$  within  $\Delta t = 13.6T$ , so that the averaged group velocity over that distance is about  $\bar{v}_g = 14.7c$ . Comparing the formation of k-gap solitons for narrow (Fig. 2a), medium (Fig. 2b) and wide (Fig. 2c) input beams, we find that  $\bar{v}_g$  of the peak is higher as the excitation beam is wider. The increased velocity of the peak comes from the larger interval the peak has to cover before it is halted by the forerunner. The simulations indicate that the k-gap soliton has infinite group velocity ( $\bar{v}_g \rightarrow \infty$ ) in the limit of plane-wave (beam of infinite width) excitation, evolving into the theoretically predicted profile (Eq. 10). In the simulations, the parameters are  $c = 1$ ,  $\delta_1 = 0.12$ ,  $\beta = 0.01$ ,  $\Omega = 4\pi$ , time is presented in units of  $2T$ , and space in the units of  $2cT$ . However, Eq. 10 implies that the infinite group velocity is a universal phenomenon that does not depend on the magnitude of the parameters, as long as they obey the relative smallness of parameters with respect to each other.

Next, we verify that this faster-than-light propagation of the k-gap soliton does not contradict Einstein's causality, by comparing the group velocity and the information velocity. The group velocity of a wavepacket is commonly defined by the motion of its center, while the information velocity is defined by the motion of the leading edge [51–53]. Generally, physical superluminality is associated with gain media where the apparent movement of the peak is created from increase in the local field by the gain, and not by actual transport of energy. This implies that the velocity of the wavefront is the relevant information velocity, rather than the velocity of the peak. [10-14, 53]. Thus, we launch a truncated Gaussian beam into the PTC, to have a clear cut on the

propagation of the information contained in the leading edge. Figure 2e shows that the truncation position (the forerunner) travels almost exactly at the speed of light in medium, but never faster. This result holds even with material dispersion  $\epsilon(\omega)$  by recalling that in the limit  $\omega \rightarrow \infty$ , the electromagnetic response is always  $\epsilon \rightarrow 1$ . The sharp edge (the forerunner) created by the truncation consists of all spatial wavenumbers, hence the forerunner always moves exactly at  $c_0$  (vacuum speed of light). As seen in Fig. 2e, the momentum constituents of the k-gap soliton never go beyond the forerunner, and the peak slows down as it approaches the forerunner. Further investigation shows that the velocity of the peak of the k-gap soliton depends on the seed's spatial profile, with wider beams displaying faster propagation before reaching the forerunner. Moreover, in principle, the soliton can arise from quantum fluctuations, as can be conjectured from recent work in quantum phenomena in PTCs [12,15]. In that case, the k-gap soliton can arise from arbitrary small noise by the amplification from the k-gap. However, even via the quantum process, the presence of the slightest signal cannot overrun the forerunner (see Fig. 2e).

**Power dependence of k-gap and threshold of amplification.** We find that the presence of the Kerr nonlinearity can alter the band structure of the PTC by shifting the k-gap to higher k-vectors, and shrinking the k-gap width. Under mean-field approximation, given  $n(t) = n_0 + n_1 \cos \Omega t + n_2 I$ , with  $n_0 = \sqrt{\epsilon_r}$ ,  $n_1 = \chi_1/2$ ,  $n_2 = \chi_3/2$ , and  $I = \frac{\epsilon_r}{2} \langle |E|^2 \rangle$  is the field intensity, one can solve the nonlinear energy band by linearizing around the k-gap (see derivation in SM), which yields

$$\omega(k, I) = \frac{\Omega}{2} \pm i\Omega \sqrt{\frac{1}{4} \left( \frac{n_1}{n_0 + n_2 I} \right)^2 \left( \frac{c_0 k / \Omega}{n_0 + n_2 I} \right)^4 - \left( \left( \frac{c_0 k / \Omega}{n_0 + n_2 I} \right)^2 - \frac{1}{4} \right)^2} \quad (12)$$

The field intensity ( $I$ ) shifts the center of the k-gap. The k-gap amplification/gain factor is given by the imaginary part of (12):  $\gamma(k, I) = |\Im(\omega(k, I))|$ , that is, different k-components experience

different gain factors. The arrest of the exponential growth occurs because, as the intensity increases, the shift in the band structure eventually brings the  $k$ -components of the soliton outside the momentum gap. A detailed explanation can be found in the Supplementary Material [58].

**Conclusion.** To summarize, we presented  $k$ -gap solitons in nonlinear PTCs, and found them to be superluminal. The faster-than-light behavior is understandable by Sommerfeld's forerunner, as tested numerically by the truncated seed beam. Importantly, the superluminal  $k$ -gap soliton does not contradict Einstein's Special Relativity. The interplay between the time-modulation and the Kerr nonlinearity gives rise to the exponential growth in time until a certain peak is reached, followed by a decaying intensity profile leading to the shape of a  $k$ -gap soliton that is always finite in its temporal width, although instability eventually leads to a train of solitons. Our results of superluminal  $k$ -gap solitons provide new insights into the study of time-varying media [54] and the gapped momentum states [55] in photonics and other time-modulated physical systems.

### **Acknowledgement**

This research was supported by a grant from the Air Force Office of Scientific Research (AFOSR).

## Appendix

### 1. Extending 1D PTCs to higher dimension PTCs by confining the transverse direction

The formulation of solitons in PTCs can be extended to two spatial dimensions, where one of them is confined in a waveguide structure in the direction transverse to the propagation direction (henceforth the "transverse dimension") and the entire index varies in time in a spatially-uniform manner. To reduce the underlying equation to the k-gap solitons described in the main text, the refractive index contrast defining the waveguide in the transverse dimension has to be larger than the temporal variations in the refractive index.

Formally, we take the conventional nonlinear wave equation for  $E$  in 2+1D PTCs,  $\nabla^2 E = \left(\frac{\partial^2}{\partial x^2} + \frac{\partial^2}{\partial y^2}\right)E = \mu_0 \frac{\partial^2}{\partial t^2}(\epsilon(y, t)E)$  with the variations both in time and in the  $y$ -direction,  $\epsilon(y, t) = \epsilon_0 \tilde{\epsilon}_r(t) \tilde{\epsilon}_r(y)$ , while keeping the  $x$ -direction uniform. Therefore, we simplify the wave equation as

$$\left(\frac{\partial^2}{\partial x^2} + \frac{\partial^2}{\partial y^2}\right)E = \frac{1}{c^2} \frac{\partial^2}{\partial t^2}(\tilde{\epsilon}_r(t) \tilde{\epsilon}_r(y)E) \quad (A1)$$

with  $\mu_0 \epsilon_0 = 1/c^2$  and  $\tilde{\epsilon}_r(t) = 1 + \delta_1 \cos \Omega t$ ,  $\tilde{\epsilon}_r(y) = 1 + \delta(y)$  are both dimensionless. In our setting, we assume both the time and spatial variations are small,  $\delta_1 \ll 1$ ,  $|\delta(y)| < 0.5 (\ll 1)$ .

It is important to note that, in order to significantly confine the field in the  $y$ -direction, we also require the spatial variation in epsilon to be stronger than the time modulation,  $|\delta(y)| > \delta_1$ . In our simulations we use  $\delta_1 \approx 0.3$ , so it is smaller than relevant values of  $\delta(y)$ , and big enough to support a substantial gap. In fact, the modulations are written in a convenient product form, which can be approximated as  $\tilde{\epsilon}_r(t) \tilde{\epsilon}_r(y) \approx 1 + \delta_1 \cos \Omega t + \delta(y)$ , where the term  $\delta_1 \delta(y)$  is negligible.

Next, we seek a solution of a separable form:  $E = f(y)E(x, t) = f(y)E_k(t)e^{ikx}$ , hence

$$\frac{c^2}{\tilde{\epsilon}_r(y)f(y)} \left(-k^2 + \frac{\partial^2}{\partial y^2}\right)f(y) = \frac{1}{E_k(t)} \frac{\partial^2}{\partial t^2}(\tilde{\epsilon}_r(t)E_k(t)) = -v^2 \quad (A2)$$

Here, two parameters are introduced: wavenumber  $k$  and frequency  $\nu$ . Then, we obtain two separable equations:

$$\begin{aligned} \left(-k^2 + \frac{\partial^2}{\partial y^2}\right) f(y) + \frac{\tilde{\epsilon}_r(y)\nu^2}{c^2} f(y) &= 0 \\ \frac{\partial^2}{\partial t^2} (\tilde{\epsilon}_r(t)E_k(t)) + \nu^2 E_k(t) &= 0 \end{aligned} \quad (A3)$$

From the first equation, we obtain the relation  $\nu = \nu(k)$  and the confined transverse profile  $f = f_{k,\nu}(y)$  in the PTC region. The second equation in Eq. (A3) is mathematically equivalent to Eq. (2) in the main text, with  $\nu(k)$  acting as a modified  $k$ -wavenumber, but with some important differences. Namely, here the equation is for the electric field  $E$ , instead of the displacement field  $D$  in the main text. Also, the equation here deals with a single  $k$ -component, whereas in the main text we use the spatial derivative. The a-priori assumption here is that the solution is separable (a wavepacket in  $y$  and multiplied by a spatiotemporal wavepacket in  $x$  and  $t$ ), Physically, this means that the solution is a guided mode (bound-state) in the  $y$ -direction, whereas in  $x$ - $t$  it is a spatiotemporal wavepacket, as it is for the 1D case. This is actually standard for experimenting with 1+1D soliton in optical Kerr media [56], where all the experiments were carried out in a slab waveguide structure. We verified that this a-priori assumption holds in the presence of nonlinearity by comparing it to an analytical solution that has only one  $k$ -component.

## 2. Steady-state linear stability analysis of nonlinear PTCs.

Consider the NLSE (Eq. 9 derived in the main text)

$$\left(-i\frac{\partial}{\partial x} - \frac{\text{GVD}}{2}\frac{\partial^2}{\partial t^2}\right)a + \alpha|a|^2a = 0 \quad (A4)$$

which takes the limit  $\nu_g \rightarrow \infty$  at the band edge of  $k$ -gap. This equation allows plane-wave (often called continuous wave (CW)) solutions. In particular, neglecting the time derivative, Eq. A4 is readily solved to obtain the steady-state CW solution in the following form:

$$a_0 = \sqrt{P_0} \exp(i\phi_{NL}) \quad (A5)$$

where  $P_0$  is the incident power and  $\phi_{NL} = -\alpha P_0 x$  is the nonlinear phase shift induced by the Kerr nonlinearity. The stability of the steady-state solution against small perturbations is determined by linearizing the following solution (G. Agrawal, Nonlinear Fiber optics, Chap 5, p. 127-129, the 6<sup>th</sup> version, Elsevier, 2019)

$$a(x, t) = (\sqrt{P_0} + \epsilon(x, t)) \exp(i\phi_{NL}). \quad (A6)$$

Here, we perturb the steady state slightly and substitute A6 into A4, resulting in the linear evolution dynamics of  $\epsilon(x, t)$  (where we keep only the leading term):

$$\left(-i \frac{\partial}{\partial x} - \frac{\text{GVD}}{2} \frac{\partial^2}{\partial t^2}\right) \epsilon + \alpha P_0 (\epsilon + \epsilon^*) = 0 \quad (A7)$$

This linear equation can be solved easily by the Fourier transform. However, because of the  $\epsilon^*$  term, the Fourier components at wavevector  $\tilde{K}$  and  $-\tilde{K}$  are coupled. Thus, we use an ansatz in the form

$$\epsilon(x, t) = \epsilon_1 \exp(i(\tilde{K}x - \tilde{\Omega}t)) + \epsilon_2 \exp(-i(\tilde{K}x - \tilde{\Omega}t)) \quad (A8)$$

where  $\tilde{K}$  and  $\tilde{\Omega}$  are the wavenumber and the frequency of perturbation, respectively. Substituting A8 into A7, we obtain two coupled equations for  $\epsilon_1$  and  $\epsilon_2$ :

$$\begin{aligned} \left(\tilde{K} + \frac{\text{GVD}}{2} \tilde{\Omega}^2 + \alpha P_0\right) \epsilon_1 + \alpha P_0 \epsilon_2^* &= 0 \\ \left(-\tilde{K} + \frac{\text{GVD}}{2} \tilde{\Omega}^2 + \alpha P_0\right) \epsilon_2 + \alpha P_0 \epsilon_1^* &= 0 \end{aligned} \quad (A9)$$

This set of two equations has a nontrivial solution only when  $\tilde{K}$  and  $\tilde{\Omega}$  satisfy the following dispersion relation

$$\tilde{K} = \pm \frac{|\text{GVD}|}{2} \tilde{\Omega} \sqrt{\tilde{\Omega}^2 + \frac{4\alpha P_0}{\text{GVD}}} = \pm \frac{|\text{GVD}\tilde{\Omega}|}{2} \sqrt{\tilde{\Omega}^2 + \text{sgn}(\text{GVD})\text{sgn}(\alpha)\tilde{\Omega}_c^2} \quad (A10)$$

where the critical frequency is defined as  $\tilde{\Omega}_c^2 = \left| \frac{4\alpha P_0}{\text{GVD}} \right|$ ,  $\text{sgn}(\text{GVD}) = \pm 1$ ,  $\text{sgn}(\alpha) = \pm 1$  depend on the signs of the group velocity dispersion and the nonlinearity, respectively. This dispersion relation shows that steady-state stability depends on whether the light seed experiences the combination of normal GVD with the focusing nonlinearity, or anomalous GVD with defocusing nonlinearity. In cases of  $\text{sgn}(\text{GVD})\text{sgn}(\alpha) = -1$ ,  $\tilde{K}$  becomes imaginary for  $\tilde{\Omega} < \tilde{\Omega}_c$ , which leads to instability. Correspondingly, the perturbation  $\epsilon(x, t)$  grows exponentially, which makes the steady-state CW solution (A5) unstable. The gain spectrum of this instability is obtained by the multiple-scale analysis as discussed in the Supplementary Material, Section 4.

## References

- [1] F. R. Morgenthaler, *Velocity Modulation of Electromagnetic Waves*, IRE Transactions on Microwave Theory and Techniques **6**, 167 (1958).
- [2] D. Holberg and K. Kunz, *Parametric Properties of Fields in a Slab of Time-Varying Permittivity*, IEEE Trans Antennas Propag **14**, 183 (1966).
- [3] J. T. Mendonça and P. K. Shukla, *Time Refraction and Time Reflection: Two Basic Concepts*, Phys Scr **65**, 160 (2002).
- [4] A. B. Shvartsburg, *Optics of Nonstationary Media*, Physics-Uspekhi **48**, 797 (2005).
- [5] F. Biancalana, A. Amann, and E. P. O'Reilly, *Gap Solitons in Spatiotemporal Photonic Crystals*, Phys Rev A (Coll Park) **77**, 11801 (2008).
- [6] J. R. Zurita-Sánchez, P. Halevi, and J. C. Cervantes-Gonzalez, *Reflection and Transmission of a Wave Incident on a Slab with a Time-Periodic Dielectric Function  $\epsilon(t)$* , Phys Rev A (Coll Park) **79**, 053821 (2009).
- [7] J. R. Reyes-Ayona and P. Halevi, *Observation of Genuine Wave Vector ( $k$  or  $\beta$ ) Gap in a Dynamic Transmission Line and Temporal Photonic Crystals*, Appl Phys Lett **107**, 074101 (2015).
- [8] A. M. Shaltout, J. Fang, A. v Kildishev, and V. M. Shalaev, *Photonic Time-Crystals and Momentum Band-Gaps*, in *CLEO: QELS\_Fundamental Science* (Optical Society of America, 2016), pp. FM1D-4.
- [9] J. S. Martínez-Romero and P. Halevi, *Parametric Resonances in a Temporal Photonic Crystal Slab*, Phys Rev A (Coll Park) **98**, 53852 (2018).
- [10] N. Wang, Z.-Q. Zhang, and C. T. Chan, *Photonic Floquet Media with a Complex Time-Periodic Permittivity*, Phys Rev B **98**, 85142 (2018).
- [11] E. Lustig, Y. Sharabi, and M. Segev, *Topological Aspects of Photonic Time Crystals*, Optica **5**, 1390 (2018).
- [12] M. Lyubarov, Y. Lumer, A. Dikopoltsev, E. Lustig, Y. Sharabi, and M. Segev, *Amplified Emission and Lasing in Photonic Time Crystals*, Science (1979) eabo3324 (2022).
- [13] Y. Sharabi, E. Lustig, and M. Segev, *Disordered Photonic Time Crystals*, Phys Rev Lett **126**, 163902 (2021).
- [14] Y. Sharabi, A. Dikopoltsev, E. Lustig, Y. Lumer, and M. Segev, *Spatiotemporal Photonic Crystals*, Optica **9**, 585 (2022).
- [15] A. Dikopoltsev, Y. Sharabi, M. Lyubarov, Y. Lumer, S. Tsesses, E. Lustig, I. Kaminer, and M. Segev, *Light Emission by Free Electrons in Photonic Time-Crystals*, Proceedings of the National Academy of Sciences **119**, e2119705119 (2022).
- [16] V. Pacheco-Peña and N. Engheta, *Temporal Aiming*, Light Sci Appl **9**, 1 (2020).
- [17] V. Pacheco-Peña and N. Engheta, *Spatiotemporal Isotropic-to-Anisotropic Meta-Atoms*, New J Phys **23**, 095006 (2021).
- [18] V. Pacheco-Peña and N. Engheta, *Temporal Equivalent of the Brewster Angle*, Phys Rev B **104**, 214308 (2021).
- [19] J. Li, Y. Li, P.-C. Cao, M. Qi, X. Zheng, Y.-G. Peng, B. Li, X.-F. Zhu, A. Alù, and H. Chen, *Reciprocity of Thermal Diffusion in Time-Modulated Systems*, Nat Commun **13**, 1 (2022).
- [20] G. Castaldi, V. Pacheco-Peña, M. Moccia, N. Engheta, and V. Galdi, *Exploiting Space-Time Duality in the Synthesis of Impedance Transformers via Temporal Metamaterials*, Nanophotonics **10**, 3687 (2021).

- [21] H. Li, S. Yin, E. Galiffi, and A. Alù, *Temporal Parity-Time Symmetry for Extreme Energy Transformations*, Phys Rev Lett **127**, 153903 (2021).
- [22] R. Maas, J. Parsons, N. Engheta, and A. Polman, *Experimental Realization of an Epsilon-near-Zero Metamaterial at Visible Wavelengths*, Nat Photonics **7**, 907 (2013).
- [23] L. Caspani, R. P. M. Kaipurath, M. Clerici, M. Ferrera, T. Roger, J. Kim, N. Kinsey, M. Pietrzyk, A. di Falco, and V. M. Shalaev, *Enhanced Nonlinear Refractive Index in  $\epsilon$ -near-Zero Materials*, Phys Rev Lett **116**, 233901 (2016).
- [24] Y. Zhou, M. Z. Alam, M. Karimi, J. Upham, O. Reshef, C. Liu, A. E. Willner, and R. W. Boyd, *Broadband Frequency Translation through Time Refraction in an Epsilon-near-Zero Material*, Nat Commun **11**, 1 (2020).
- [25] V. Bruno, C. DeVault, S. Vezzoli, Z. Kudyshev, T. Huq, S. Mignuzzi, A. Jacassi, S. Saha, Y. D. Shah, and S. A. Maier, *Negative Refraction in Time-Varying Strongly Coupled Plasmonic-Antenna-Epsilon-near-Zero Systems*, Phys Rev Lett **124**, 043902 (2020).
- [26] V. Bruno, S. Vezzoli, C. DeVault, E. Carnemolla, M. Ferrera, A. Boltasseva, V. M. Shalaev, D. Faccio, and M. Clerici, *Broad Frequency Shift of Parametric Processes in Epsilon-near-Zero Time-Varying Media*, Applied Sciences **10**, 1318 (2020).
- [27] E. Lustig, S. Saha, E. Bordo, C. DeVault, S. N. Chowdhury, Y. Sharabi, A. Boltasseva, O. Cohen, V. M. Shalaev, and M. Segev, *Towards Photonic Time-Crystals: Observation of a Femtosecond Time-Boundary in the Refractive Index*, in *2021 Conference on Lasers and Electro-Optics (CLEO) (IEEE, 2021)*, pp. 1–2.
- [28] R. Tirole, E. Galiffi, J. Dranczewski, T. Attavar, B. Tilmann, Y.-T. Wang, P. A. Huidobro, A. Alú, J. B. Pendry, and S. A. Maier, *Saturable Time-Varying Mirror Based on an ENZ Material*, ArXiv Preprint ArXiv:2202.05937 (2022).
- [29] X. Wang, M. S. Mirmoosa, V. S. Asadchy, C. Rockstuhl, S. Fan, and S. A. Tretyakov, *Metasurface-Based Realization of Photonic Time Crystals*, ArXiv Preprint ArXiv:2208.07231 (2022).
- [30] W. Chen and D. L. Mills, *Optical Response of Nonlinear Multilayer Structures: Bilayers and Superlattices*, Phys Rev B **36**, 6269 (1987).
- [31] W. Chen and D. L. Mills, *Gap Solitons and the Nonlinear Optical Response of Superlattices*, Phys Rev Lett **58**, 160 (1987).
- [32] J. E. Sipe and H. G. Winful, *Nonlinear Schrödinger Solitons in a Periodic Structure*, Opt Lett **13**, 132 (1988).
- [33] A. B. Aceves and S. Wabnitz, *Self-Induced Transparency Solitons in Nonlinear Refractive Periodic Media*, Phys Lett A **141**, 37 (1989).
- [34] D. N. Christodoulides and R. I. Joseph, *Slow Bragg Solitons in Nonlinear Periodic Structures*, Phys Rev Lett **62**, 1746 (1989).
- [35] B. J. Eggleton, R. E. Slusher, C. M. de Sterke, P. A. Krug, and J. E. Sipe, *Bragg Grating Solitons*, Phys Rev Lett **76**, 1627 (1996).
- [36] D. N. Christodoulides and R. I. Joseph, *Discrete Self-Focusing in Nonlinear Arrays of Coupled Waveguides*, Opt Lett **13**, 794 (1988).
- [37] Y. S. Kivshar, *Self-Localization in Arrays of Defocusing Waveguides*, Opt Lett **18**, 1147 (1993).
- [38] H. S. Eisenberg, Y. Silberberg, R. Morandotti, A. R. Boyd, and J. S. Aitchison, *Discrete Spatial Optical Solitons in Waveguide Arrays*, Phys Rev Lett **81**, 3383 (1998).

- [39] N. K. Efremidis, S. Sears, D. N. Christodoulides, J. W. Fleischer, and M. Segev, *Discrete Solitons in Photorefractive Optically Induced Photonic Lattices*, Phys Rev E **66**, 46602 (2002).
- [40] J. W. Fleischer, M. Segev, N. K. Efremidis, and D. N. Christodoulides, *Observation of Two-Dimensional Discrete Solitons in Optically Induced Nonlinear Photonic Lattices*, Nature **422**, 147 (2003).
- [41] J. W. Fleischer, T. Carmon, M. Segev, N. K. Efremidis, and D. N. Christodoulides, *Observation of Discrete Solitons in Optically Induced Real Time Waveguide Arrays*, Phys Rev Lett **90**, 23902 (2003).
- [42] F. Lederer, G. I. Stegeman, D. N. Christodoulides, G. Assanto, M. Segev, and Y. Silberberg, *Discrete Solitons in Optics*, Phys Rep **463**, 1 (2008).
- [43] D. J. Kaup and A. C. Newell, *On the Coleman Correspondence and the Solution of the Massive Thirring Model*, Lett. Nuovo Cim **20**, 325 (1977).
- [44] S. Coleman, *Quantum Sine-Gordon Equation as the Massive Thirring Model, in Bosonization* (World Scientific, 1994), pp. 128–137.
- [45] S. v Manakov, *On the Theory of Two-Dimensional Stationary Self-Focusing of Electromagnetic Waves*, Soviet Physics-JETP **38**, 248 (1974).
- [46] C. R. Menyuk, *Stability of Solitons in Birefringent Optical Fibers. I: Equal Propagation Amplitudes*, Opt Lett **12**, 614 (1987).
- [47] S. G. Evangelides, L. F. Mollenauer, J. P. Gordon, and N. S. Bergano, *Polarization Multiplexing with Solitons*, Journal of Lightwave Technology **10**, 28 (1992).
- [48] R. Radhakrishnan, M. Lakshmanan, and J. Hietarinta, *Inelastic Collision and Switching of Coupled Bright Solitons in Optical Fibers*, Phys Rev E **56**, 2213 (1997).
- [49] J. U. Kang, G. I. Stegeman, J. S. Aitchison, and N. Akhmediev, *Observation of Manakov Spatial Solitons in AlGaAs Planar Waveguides*, Phys Rev Lett **76**, 3699 (1996).
- [50] C. Anastassiou, M. Segev, K. Steiglitz, J. A. Giordmaine, M. Mitchell, M. Shih, S. Lan, and J. Martin, *Energy-Exchange Interactions between Colliding Vector Solitons*, Phys Rev Lett **83**, 2332 (1999).
- [51] A. Sommerfeld, *Über Die Fortpflanzung Des Lichtes in Dispergierenden Medien*, Ann Phys **349**, 177 (1914).
- [52] L. Brillouin, *Über Die Fortpflanzung Des Lichtes in Dispergierenden Medien*, Ann Phys **349**, 203 (1914).
- [53] L. J. Wang, A. Kuzmich, and A. Dogariu, *Gain-Assisted Superluminal Light Propagation*, Nature **406**, 277 (2000).
- [54] E. Galiffi, R. Tirole, S. Yin, H. Li, S. Vezzoli, P. A. Huidobro, M. G. Silveirinha, R. Sapienza, A. Alù, and J. B. Pendry, *Photonics of Time-Varying Media*, ArXiv Preprint ArXiv:2111.08640 (2021).
- [55] M. Baggioli, M. Vasin, V. Brazhkin, and K. Trachenko, *Gapped Momentum States*, Phys Rep **865**, 1 (2020).
- [56] J. S. Aitchison, A. M. Weiner, Y. Silberberg, M. K. Oliver, J. L. Jackel, D. E. Leaird, E. M. Vogel, and P. W. E. Smith, *Observation of Spatial Optical Solitons in a Nonlinear Glass Waveguide*, Opt Lett **15**, 471 (1990).
- [57] G. P. Agrawal, *Nonlinear Fiber Optics*, in *Nonlinear Science at the Dawn of the 21st Century* (Springer, 2000), pp. 195–211.

- [58] See Supplemental Material [[url](#)] for full derivations of nonlinear PTCs, a train of k-gap solitons, and intensity dependence of the k-gapped band structure, which includes Refs. [59-72].
- [59] P. D. Drummond and M. Hillery, *The Quantum Theory of Nonlinear Optics* (Cambridge University Press, 2014).
- [60] N. Quesada and J. E. Sipe, *Why You Should Not Use the Electric Field to Quantize in Nonlinear Optics*, *Opt Lett* **42**, 3443 (2017).
- [61] M. Born and L. Infeld, *Foundations of the New Field Theory*, Proceedings of the Royal Society of London. Series A, Containing Papers of a Mathematical and Physical Character **144**, 425 (1934).
- [62] J. T. Mendonça, G. Brodin, and M. Marklund, *Vacuum Effects in a Vibrating Cavity: Time Refraction, Dynamical Casimir Effect, and Effective Unruh Acceleration*, *Phys Lett A* **372**, 5621 (2008).
- [63] A. Hasegawa, *Generation of a Train of Soliton Pulses by Induced Modulational Instability in Optical Fibers*, *Opt Lett* **9**, 288 (1984).
- [64] D. Anderson and M. Lisak, *Modulational Instability of Coherent Optical-Fiber Transmission Signals*, *Opt Lett* **9**, 468 (1984).
- [65] K. Tai, A. Hasegawa, and A. Tomita, *Observation of Modulational Instability in Optical Fibers*, *Phys Rev Lett* **56**, 135 (1986).
- [66] M. J. Potasek, *Modulation Instability in an Extended Nonlinear Schrödinger Equation*, *Opt Lett* **12**, 921 (1987).
- [67] G. P. Agrawal, P. L. Baldeck, and R. R. Alfano, *Modulation Instability Induced by Cross-Phase Modulation in Optical Fibers*, *Phys Rev A (Coll Park)* **39**, 3406 (1989).
- [68] S. Trillo and S. Wabnitz, *Dynamics of the Nonlinear Modulational Instability in Optical Fibers*, *Opt Lett* **16**, 986 (1991).
- [69] L. F. Mollenauer, R. H. Stolen, and J. P. Gordon, *Experimental Observation of Picosecond Pulse Narrowing and Solitons in Optical Fibers*, *Phys Rev Lett* **45**, 1095 (1980).

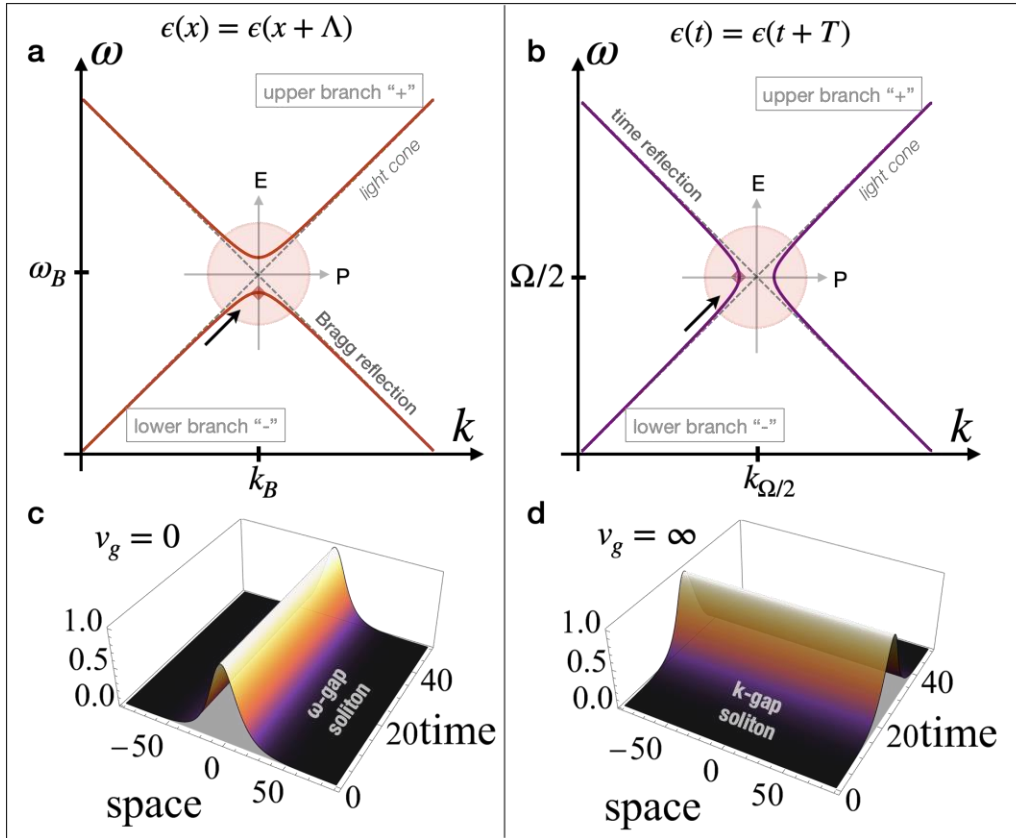


Fig. 1: (a) Band structure of a PC created by spatial periodic modulation  $\epsilon(x) = \epsilon(x + \Lambda)$ . (b) Band structure of a PTC created by the temporal periodic modulation  $\epsilon(t) = \epsilon(t + T)$ . (c) Self-focusing Kerr nonlinearity gives rise to a Bragg ( $\omega$ -gap) soliton emerging at the band edge where the group velocity ( $v_g$ ) is zero. (d) Self-focusing Kerr nonlinearity gives rise to a  $k$ -gap soliton emerging at the band edge where the group velocity is infinite.

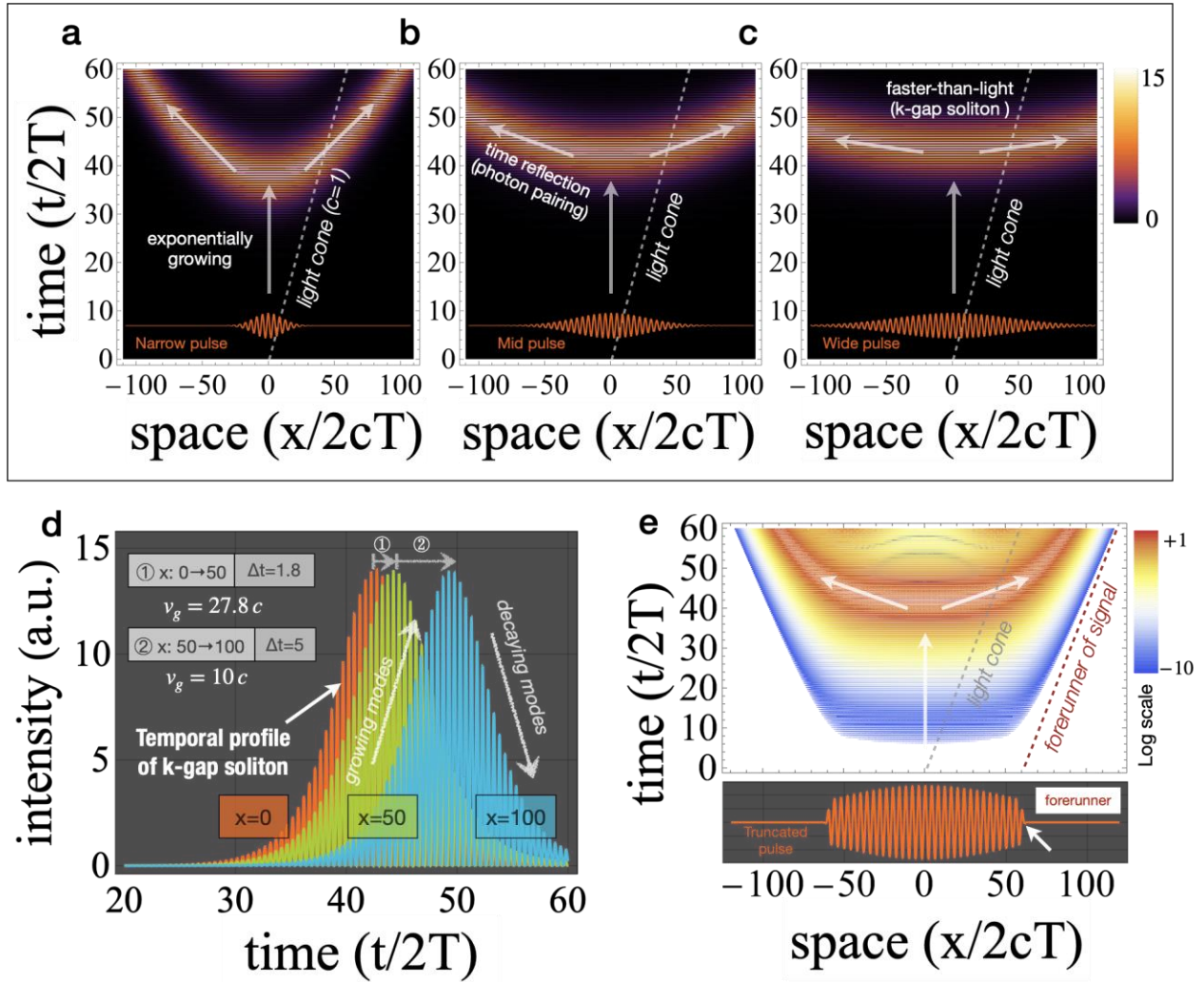


Fig. 2: (a-c) Generation of a k-gap soliton from an input of (a) narrow, (b) mid, and (c) wide beams, respectively. (d) The temporal profiles of the k-gap solitons at different locations ( $x = 0, 50, 100$  [ $2cT$ ]) found numerically from the seed beam in (b). This soliton exhibits superluminal behavior with effective average group velocity of  $v_g = 14.7c$ . (e) Evolution of a truncated beam with a central wave vector ( $k_0$ ) at the middle of the k-gap. The truncation mimics the forerunner of signal velocity, instead of the center-of-mass light cone. Once formed, the k-gap soliton travels faster than light in medium, but still slower than the forerunner of the information in the leading edge. The peak (which is also the "center of mass") of the k-gap soliton always slows down before it hits the forerunner, as indicated in (d) by the slowing down of the effective group velocity from its value in the section  $x = 0$  to  $x = 50$ , to a smaller value in the section  $x = 50$  to  $x = 100$ .